# The olivary input to the cerebellum dissociates sensory events from movement plans

Jay S. Pi[1], Mohammad Amin Fakharian[1], Paul Hage[1], Ehsan Sedaghat-Nejad[1], Salomon Z. Muller[2], and Reza Shadmehr[1]

[1]Laboratory for Computational Motor Control, Dept. of Biomedical Engineering, Johns Hopkins School of Medicine, Baltimore, Maryland 21205, USA

[2]Zuckerman Mind Brain Behavior Institute, Department of Neuroscience, Columbia University, New York, NY 10027, USA

**Correspondence**: Reza Shadmehr or Jay S. Pi, Johns Hopkins School of Medicine, 410 Traylor Building, 720 Rutland Ave., Baltimore, MD 21205.
Email: shadmehr@jhu.edu or jay.s.314159@gmail.com

**Acknowledgements:** The work was supported by grants from the National Science Foundation (CNS-1714623), the NIH (R01-EB028156, R01-NS078311), and the Office of Naval Research (N00014-15-1-2312).

**Author contributions:** J.S.P., E.S.H, P.H., and R.S. conceived and performed experiments. J.S.P., E.S.N., M.A.F., and R.S. analyzed data, J.S.P. made figures and performed statistical analysis. R.S. and S.Z.M. wrote the manuscript.

**Competing interests:** None.

**Abstract**

The inferior olive is thought to act as an instructor that mentors the Purkinje cells (P-cells) of the cerebellum. As a result, if during a behavior two groups of P-cells received different kinds of information from their olivary inputs, then each group might contribute to different aspects of that behavior. Here, we designed a saccade task in marmosets that dissociated sensory and motor events and then recorded the complex and simple spikes of hundreds of P-cells. We found that the olivary input to one group of P-cells robustly reported the direction of the random visual target, whereas the input to another group principally reported the spatial properties of the forthcoming movement. When a saccade encountered a sensory prediction error, but the subject chose not to make a corrective movement, the error was reported to the first group of P-cells, not the second group. In the first group the simple spikes were suppressed during fixation, then produced a burst before saccade onset that acted primarily as an agonist which accelerated the movement. In the second group the simple spikes were not suppressed during fixation and did not provide an agonist assistance. Rather, the simple spikes acted as an antagonist that decelerated the movement. Therefore, the olive differentiated the P-cells based on whether they would receive primarily sensory or motor information, and this dissociated their contributions to both control of movements and holding still.

Significance statement

The inferior olive provides more than just error information to the P-cells: it also informs them regarding the spatial properties of forthcoming movements. However, these two kinds of information are sent to two different groups of cells. The P-cells whose olivary input directionally report a visual event have a simple spike response that accelerates the saccade toward that same direction. The P-cells whose olivary input directionally predicts a forthcoming movement have a simple spike response that decelerates the saccade in that same direction.

## Introduction

Theories of cerebellar function suggest that we learn how to move because the inferior olive provides a teaching signal to the Purkinje cells (P-cells) of the cerebellum (*1–3*). This signal results in complex spikes (CS) which encode a prediction error (*3–5*) that then trains the simple spikes (SS) (*3*, *6*), the output of P-cells. However, the occurrence of an error is not the only event that modulates the CS rates (*7*): while the rates are modulated following a variety of sensory events (*8–13*), they are also modulated before a variety of movements that are voluntary (*14–18*) and thus are not errors. For example, the CS rates are modulated by sensory events such as the touch of a limb (*19*), an air puff to the face (*10*, *11*, *20*), or sudden presentation of a visual stimulus (*9*, *21*), signaling that a salient sensory event has occurred (*10*, *13*), particularly one that is rewarding (*12*). But the CS rates are also modulated before voluntary movements such as walking (*16*), licking (*14*), reaching (*8*, *15*, *17*, *18*, *22*), and moving the wrist (*23*), none of which are errors. This rich diversity of events that affect the CS rates begs the question: what information is encoded in the climbing fiber input to the cerebellum, and what is its function?

Inspired by the behavioral experiments of Wallman and Fuchs (*24*), and Tseng et al. (*25*), we designed a 2x2 saccade task in which a visual event was sometimes but not always followed by a movement, and a movement that was sometimes but not always preceded by a visual event. At the conclusion of some movements the subject experienced an error. We used reward to assign a value to this error, affording the subject the opportunity to respond to that error by making a corrective movement, or simply observe the error but withhold the movement. This allowed us to quantify the CS response to visual events, motor events, and errors that did or did not inspire corrective actions.

We recorded spiking activities of hundreds of P-cells in the oculomotor vermis of marmosets and found that following the presentation of a visual target at a random direction, the olive reported to the cerebellum the direction of that target with low latency (60 ms), and then at 10 ms before the saccade it also reported the direction of the forthcoming movement, even when the saccade was not toward the target. However, the CS response of individual P-cells differentiated two populations: in one group (Type 1) the CS rates encoded the direction of the target, whereas in another group (Type 2) the CS rates encoded the direction of the forthcoming movement.

At the conclusion of some saccades the target was not on the fovea, indicating a sensory prediction error. On trials in which the subject chose to make a corrective movement the CS response strongly encoded the error direction in both groups of P-cells. However, if the subject chose to withhold the movement, the error information was still transmitted from the olive to the cerebellum, but only to the Type 1 cells. That is, the olive reported sensory prediction errors to only one group of P-cells.

If we view the olivary signal as a teacher, then because these two groups are mentored differentially, we expect that they might contribute to distinct aspects of behavior. Thus, we considered the SSs that we recorded simultaneously with the CSs and found that the P-cells whose olivary input directionally encoded the visual target had an SS response that accelerated saccades toward that same direction. In contrast, the P-cells whose olivary input directionally encoded the forthcoming movement had an SS response that decelerated saccades in that same direction.

## Results

Marmosets fixated a center location and were presented with a primary target at a random direction (Fig. 1A). As the primary saccade commenced, we moved the target to a random secondary location,

thus inducing a sensory prediction error that was usually corrected by a movement (Fig. 1B). To assign a value to this error, in 60% of the sessions reward required both the primary and the secondary saccades (Fig. 1A, left subplot), whereas in the remaining sessions reward required only the primary saccade (Fig. 1A, right subplot). If reward did not require the secondary saccade, the secondary target was presented briefly (~120 ms, adjusted during the recording session) and then returned to the primary location. Following fixation of the final target, the center target was presented, and the subject made a center saccade. Thus, the 2x2 design allowed us to differentiate between responses to visual events, motor events, and sensory prediction errors that followed a movement but may or may not inspire a corrective movement.

We combined MRI and CT guided targeting procedures (*26*) to place tetrodes, heptodes, and silicon probes in lobules VI and VII of the vermis and recorded from n=389 P-cells over a 2.5 year period in n=2 marmosets. In every case, the neuron was identified as a P-cell because of the presence of CSs. In n=257 P-cells we isolated both the SSs and the CSs and confirmed that the CS suppressed the SS. The data set for each P-cell included an average of 1900 task-relevant saccades to visual targets and an additional 2200 task irrelevant saccades.

In general, the SS response, as exemplified in the four P-cells shown in Figs. 1D & 1E, varied widely between the cells (*5*, *27*, *28*). For example, during the primary saccade, cell 1 exhibited a pause-burst pattern, cell 2 exhibited a burst pattern, cell 3 exhibited a pause pattern, and cell 4 exhibited a burst-pause pattern. However, despite these diverse SS modulations, cells 1, 3, and 4 all had their largest CS response before saccades in direction -45$^{o}$ (termed CS-on, (*9*)). We used the CS-on direction of a P-cell to define a coordinate system for that cell (*5*, *6*, *29*). As a result, for cells 1, 3, and 4, the saccade toward 0$^{o}$ was labeled as CS+45$^{o}$, whereas the same saccade for cell 2 was labeled as CS+135$^{o}$.

*The olivary input reported the direction of the visual target and the direction of the forthcoming saccade*

We measured the CS response of each P-cell to target presentation and labeled the direction that produced the largest rate increase as CS-on (Fig. 2A, and Fig. S1A). The CS-on direction remained consistent regardless of whether it was measured in response to the primary target, the secondary target, or the center target (Fig. S1C). Notably, the CS-on direction varied approximately with the cell's location in the vermis (Fig. S1B) (*9*, *29*). P-cells on the right side of the vermis tended to have their largest CS response to visual events to the left of fovea, whereas the P-cells on the left side produced a CS in response to events on the right.

The subject was fixating the center target when the primary target was displayed at a random direction. If the target was in direction CS-on, the population displayed a sharp CS rate increase at 62 ms latency (Fig. 2A, top row), but if the target was in direction CS+180 the rates were suppressed at 85 ms latency. In contrast to the sudden changes following the visual event, the rates increased gradually before the movement in direction CS-on, reaching a peak around 10 ms before saccade onset, and decreased gradually in direction CS+180, reaching a minimum around 22 ms before saccade onset. Notably, the CS rates continued to be modulated during the saccade.

We divided the trials based on reaction times (RT) and found that the timing of the CS response to the visual event continued to express a peak at around 60 ms (Fig. 2A, 2$^{nd}$ row). However, with long RT the magnitude of the peaks after target presentation and before saccade onset both declined. Thus,

this initial analysis suggested that the olive informed the P-cells that a stimulus was presented at a particular part of the visual space, and that a saccade was about to be made toward that direction.

To test whether the olivary input independently reported the visual event and the motor plan, we considered trials in which the target was presented but the subject chose to saccade elsewhere (defined as saccades not directed to within 45$^{o}$ of the target). For this analysis, we combined the saccades that were made in response to either the primary or the secondary target. For these saccades, the time between target onset and saccade onset was 350±360 ms, long enough to dissociate the CS response to each event.

We found that the initial CS response reported the target location, not the direction of the forthcoming saccade (average firing rate in direction CS-on vs. CS-off; Wilcoxon signed rank test; target: $z=7.52$ $p=5x10^{-14}$; saccade: $z=1.62$ $p=0.1$). However, the response before the movement reported the direction of the forthcoming saccade, not the direction of the instructed target (Fig. 2B, average firing rate in direction CS-on vs. CS-off; Wilcoxon signed rank; target: $z=0.3$ $p=0.76$; saccade: $z=8.18$ $p=3x10^{-16}$).

We next asked whether the olivary input reported the direction of the forthcoming saccade even if that movement was not in response to a visual target. In task irrelevant saccades the movement was performed outside of the context of the task: the subject was not fixating the center target, and there were no sudden or unexpected sensory events that we know of that inspired these movements. Strikingly, the CS rates were modulated before the saccades and carried information regarding the direction of the movement (Fig. 2C). However, the CS rates in these task irrelevant movements were significantly less modulated as a function of direction than for task relevant saccades (vs. primary saccade, 50 ms period before saccade onset, Wilcoxon signed rank test, $z= 8.04$ $p<10^{-6}$).

In summary, the olivary input provided information regarding the direction of the visual stimulus, and then independently regarding the direction of the forthcoming movement, even when the movement was not toward the stimulus. The information regarding movement direction was still present but weaker when the saccade was not in response to the onset of a reward relevant stimulus.

*The olivary input dissociated two groups of P-cells*

The CS rate modulation in response to the primary target resembled the activities of visuomotor neurons in the superior colliculus: a sharp response after target onset, followed by ramping activity that peaked before saccade onset (*30*). In the superior colliculus, neurons in the superficial layers respond primarily to visual events, while neurons in the deeper layers respond primarily to movements (*30–32*). We wondered whether the olivary input might send visual and motor information to different P-cells.

Following the display of the primary target in direction CS-on, in one group of P-cells (Type 1, n=194) there was a sharp CS response at ~60 ms latency, but in the second group (Type 2, n=195) this visual response was absent (Fig. 3A). However, in both groups the CS rates increased in direction CS-on and reached a peak before saccade onset. Notably, whereas in Type 1 cells the CS rates dropped to near baseline around saccade onset, in the Type 2 cells the CS rates remained elevated until after saccade end. The visual response hinted that the olivary input reported the visual event principally to Type 1 cells. To check for this, we examined trials in which the subject was presented with a visual target but chose to saccade elsewhere.

In the Type 1 cells but not Type 2 cells, after target onset (30-130 ms period) the CS rates demonstrated a better encoding of target direction as compared to saccade direction (Fig. 3B, difference

in the CS-on response, target minus saccade; Wilcoxon signed rank test; Type 1 $z=3.4$ $p=3.33\times10^{-4}$, Type 2 $z=1.55$ $p=0.06$). However, before the saccade this information encoding reversed: at -110 to -10 ms before saccade onset in the Type 2 cells but not Type 1 cells the CS rates displayed a better dissociation of saccade direction vs. target direction (difference in the CS-on response, saccade minus target; Wilcoxon signed rank test; Type 2 $z=2.83$ $p=2.32\times10^{-2}$; Type 1 $z=1.37$ $p=0.08$). A follow up analysis showed that the olivary input to the Type 1 cells better encoded target direction rather than saccade direction (difference in target CS-on and saccade CS-on responses, target onset period vs. saccade onset period; Wilcoxon signed rank test $z=4.24$ $p=1\times10^{-5}$). In contrast, the olivary input to the Type 2 cells better encoded saccade direction rather than target direction (difference in saccade CS-on and target CS-on responses, saccade onset period vs. target onset periods; Wilcoxon signed rank test $z=2.98$ $p=1\times10^{-3}$).

We estimated that based on our MRI of the subject's cerebellum and the trajectory of the electrode, most of the Type 1 cells were located in the anterior part of lobule VII, whereas most of the Type 2 cells were located in the posterior part of lobule VI.

In summary, one group of P-cells (Type 1) received information from the olive principally concerning the direction of the visual target, while another group (Type 2) received information principally concerning the direction of the forthcoming movement.

*Sensory prediction error was transmitted to only the Type 1 P-cells*

Following the completion of the primary saccade, the target was not on the fovea, resulting in a sensory prediction error. We used reward to assign a value to this error: in some sessions reward required a correction, i.e., a secondary saccade, whereas in other sessions the subject had the option of withholding the corrective movement (in these trials reward required only the primary saccade). We then labeled the trials across all sessions based on whether the animal chose to make the correction or not.

We began with trials in which the subject chose to correct for the error, i.e., produce a secondary saccade. If the secondary target was in direction CS-on, and the subject chose to correct the error, in Type 1 cells we found that the CS rates peaked at around 60 ms latency (Fig. 4A, 1$^{st}$ row). Notably, this short-latency visual response was missing in Type 2 cells, confirming what we had seen in response to the primary target (Fig. 3A). If the error was in direction CS+180, both groups exhibited CS suppression that reached a peak around 100 ms following target onset. Thus, the CS response to the secondary target was similar in timing to the response that the cells had produced following the onset of the primary target. This is consistent with the fact that both the primary and secondary targets were random and thus constituted sensory prediction errors.

Critically, if the subject chose to suppress the corrective movement (Fig. 4A, 2$^{nd}$ row), then in the Type 2 cells the CS rates no longer reported the direction of error. This confirms our conclusions in Fig. 3 that the Type 2 group received olivary input that principally reported on an upcoming movement, not the visual event. As a result, without the corrective movement the sensory prediction error was insufficient to drive the olivary inputs to these P-cells. In contrast, in Type 1 cells, even without the corrective movement the presence of the error was sufficient to modulate the CS rates (CS-on vs. CS-off, 0-100ms post target onset, Wilcoxon signed rank test; $z=3.27$ $p=5\times10^{-4}$), though this modulation was

much weaker than when the error was followed by a correction (vs. error corrected, CS-on, 0-100ms post target onset; Wilcoxon signed rank test; $z=3.41$ $p=3x10^{-4}$).

As a control, we examined saccades that did not encounter an error. Two prominent examples were the secondary and center saccades (endpoint error; secondary saccade: 0.54±0.37 deg, mean±SD; center saccade: 0.85±0.5 deg). We found that before both the secondary and the center saccades the CS rates reported the direction of the forthcoming movement (Fig. 4B). However, this directionally dependent modulation stopped shortly after the saccade end (Wilcoxon signed rank test; CS-on vs. CS-off; secondary saccade, 25-75ms post saccade end, Type 1: $z=1.06$ $p=0.15$, Type 2: $z=0.50$ $p=0.31$; center saccade, 75-100ms post saccade end, Type 1: $z=0.80$ $p=0.21$, Type 2: $z=0.15$ $p=0.44$).

Thus, at the conclusion of the primary saccade the subject experienced a sensory prediction error. If it chose to suppress the corrective movement, the olive reported the direction of that error to the Type 1 cells, but not the Type 2 cells.

*Omission of an expected sensory event appeared to suppress CSs in the Type 1 cells*

The expected sensory consequence of a saccade is that the target will be on the fovea. Thus, at the end of the primary saccade, as the target was placed at a new location, the expected sensory event at the fovea was missing. If the olivary input transmitted prediction errors, and not just sensorimotor events, then this omission by itself should leave its mark in the CS activities. Thus, we asked if Type 1 cells, which responded to the presentation of the visual target, also responded to the omission of the visual target.

To directly test for this idea, we needed a condition in which the saccade ended but the target was blanked (and not moved elsewhere). We did not have such a condition. To approximate this situation, we aligned the data based on the direction of the primary saccade, and then averaged across all secondary target locations. As a control, we considered saccades that did not experience endpoint errors, i.e., the secondary and center saccades. As a further control we estimated a 95% confidence interval on post-saccadic CS rates via bootstrapping: we replaced the direction of the primary saccade with a random direction (Fig. 4C).

In general, regardless of whether there was an error at the end of a saccade or not, following a saccade (in any direction) the CS rates were suppressed below baseline (Fig. 4C). However, in Type 1 cells (but not Type 2), the CS suppression was tuned as a function of the direction of the primary saccade: the maximum CS suppression occurred following primary saccades that were in direction CS-on (comparison with bootstrap distribution, $p<1x10^{-3}$).

To confirm that this was a response to the omission of the target rather than a generic post-saccade response, we checked and found that the CS response did not exhibit a directional tuning for saccades that did not experience error (secondary and center saccades). These results suggest, but do not prove, that at the conclusion of the primary saccade, the omission of the target on the fovea may be an event that by itself generates an error signal, resulting in the suppression of the CS rates.

*Simple spikes were suppressed during fixation and then exhibited an agonist-antagonist burst during saccades*

Given that a major function of the inferior olive is to serve as a teacher for the cerebellum, it is possible that the P-cells which were mentored via visually sensitive signals (Type 1) might contribute differently

to control of behavior than P-cells which were mentored via movement sensitive signals (Type 2). Thus, we turned to the SSs that we had simultaneously recorded with the CSs.

We began by considering SS activity in the entire population, rather than cell groups. During fixation of the center target, the SS rates were suppressed below baseline (Fig. 5A, first row, Wilcoxon signed rank test; -50 to 50ms post target onset, CS-on: z=4.34 p=7x$10^{-6}$; CS-off: z=4.11 p=2x$10^{-5}$). Following presentation of the primary target, the SS rates did not exhibit a sharp change (unlike the CS response). Indeed, even in long RT trials the SS rates remained suppressed during fixation and did not appear to respond to the target presentation (Fig. 5A, 2nd row). However, near saccade onset there was a sharp increase in the SS rates. Notably, the burst was stronger and earlier if the saccade was in direction CS+180 (peak at ~20 ms before saccade onset) as compared to direction CS-on (~10 ms before saccade onset, Wilcoxon signed rank test, CS-off vs. CS-on, -20ms pre target onset, z=3.61 p=2x$10^{-4}$).

When a saccade took place in an arbitrary direction (Fig. 5B, left panel), for one group of P-cells that saccade was in direction CS-on, while for another group that same saccade was in direction CS+180. During the saccade the SSs produced by these two groups are likely to have downstream effects that oppose one another. This is because when the SSs of a P-cell are briefly suppressed during a saccade (because of arrival of a CS), the result is downstream motor commands that pull the eyes in direction CS-on of that P-cell (*33*). Similarly, when the SSs are activated via optogenetics, the result is downstream commands that pull the eyes roughly in direction CS+180 (*34*). Thus, if the saccade is in direction CS+180 of a group of P-cells, then the SSs produced by those cells are functionally the agonist of that saccade, commanding downstream forces that aid acceleration. On the other hand, if the saccade is in direction CS-on of a group of P-cells, then the SSs are functionally the antagonist, commanding downstream forces that produce deceleration. In this framework, the population response is measured by subtracting the SS rates in direction CS-on from the SS rates in direction CS+180. When we did this, the result unmasked a striking pattern: an agonist burst that preceded saccade onset, followed by an antagonist burst that reached its peak roughly 10 ms before deceleration onset (Fig. 5B, 1st row).

As the motivational state of the subject changed, so did saccade peak velocity (*35*). We measured peak velocity as a function of saccade amplitude in each subject and then normalized the data to compute vigor of each saccade (*36*, *37*). For high vigor saccades, there was no change in the agonist SS burst, but there was an increase in the antagonist burst around the time that the saccade began decelerating (Fig. 5B, 2nd row, Wilcoxon signed rank test; from -75 to -25ms of deceleration onset, z=0.543 p=0.59; from -10 to 20ms of deceleration onset, z=-3.22 z=1x$10^{-3}$).

In summary, the SSs were suppressed during fixation, then produced a burst that was earlier and stronger when the saccade was in direction CS+180, weaker and later when the saccade was in direction CS-on. The population response was an agonist burst that preceded saccade onset, followed by an antagonist burst that reached its peak just before deceleration onset.

*Both simple and complex spikes became more synchronized during saccades*

Our data included n=289 pairs of P-cells in which the CSs were isolated in both cells, and n=84 pairs of P-cells in which both the CSs and SSs were isolated in all cells. To ask whether there was a significant temporal coordination among the spikes, we computed $\Pr(A(t) = 1|B(0) = 1)$, i.e., the probability of spiking in neuron A at time t, given that neuron B spiked at time 0 (using a 1 ms time bin). Because this quantity varied with the firing rates and those rates were modulated by the task, we used interval

jittering (20 ms intervals) to randomly move the spikes without altering their average firing rates (*38*). By repeating the jittering 1000 times, we computed a 99% confidence interval (CI). This allowed us to compare the measured values with that expected from chance.

We found that if a CS occurred in one P-cell, then there was roughly 5 times greater than chance probability that the second P-cell would also produce a CS during the same 1 ms bin (Fig. 5C). This probability remained greater than chance at ±1 ms delay, but then returned to chance levels at ±2 ms delay. When an SS occurred in one P-cell, then there was roughly 1.3 times greater than chance probability that the second P-cell would also produce an SS during the same time bin. This probability returned to chance at ±1 ms delay. Thus, the CSs and SSs were on average 5 times and 1.3 times more likely to be synchronous than expected by chance.

We next asked whether the probability of synchronous spiking was modulated by the task. To compute the probability of a synchronous event with respect to chance, we used the approach suggested in (*39*): we aligned the trials to target onset or movement onset and then for each time bin computed the following quantity:

$$s(t) = \Pr(A(t) = 1, B(t) = 1) - \Pr(A(t) = 1)\Pr(B(t) = 1) \qquad (1)$$

In the above equation, $\Pr(A, B)$ is the "raw" probability of synchronous spiking, while $\Pr(A)\Pr(B)$ is the expected synchrony if the two neurons were independent. $\Pr(A)$ and $\Pr(B)$ are the measured probability of spiking in each neuron at that time bin (reflecting the average firing rate). For this analysis, we used a 1 ms bin to label a synchronous SS event, and a 4 ms bin to label a synchronous CS event. Thus, $s(t)$ quantified the probability of synchrony with respect to chance. To ask if there were task related changes in synchrony, for each cell pair we measured synchrony with respect to baseline, $s(t) - s_0$, where $s_0$ is baseline synchrony in that cell pair ($s_0$ is a constant measured during a task irrelevant period of the task, see Methods).

For the SSs both the raw synchrony $\Pr(A, B)$ and the chance synchrony $\Pr(A)\Pr(B)$ increased (Fig. 5D) near the onset of the primary saccade, as would be expected because of the increase in the firing rates. However, the observed synchrony rose faster than expected from chance, and thus at around 50 ms before saccade onset the quantity $s(t)$ began to rise and reached a peak just before saccade deceleration (Fig. 5E, Wilcoxon signed rank test, -20 to 0ms pre saccade deceleration, z=3.32 $p=5\times10^{-4}$). Moreover, during fixation of the center target, while the SS rates were suppressed, SS synchrony was reduced by an amount that was greater than expected by chance (Wilcoxon signed rank test, -50 to 50ms post target onset, z=1.89 p=0.03).

The CSs also exhibited task related synchrony. Following presentation of the primary target in direction CS-on, CS synchrony increased, reaching a peak at around 100 ms (Fig. 5F, 1st row, Wilcoxon signed rank test, 0-200ms post target onset, z=2.25 p=0.01). Similarly, before the onset of the primary saccade, CS synchrony increased, reaching a peak just before deceleration onset (-200 to 0ms pre saccade onset, z=2.38 $p=9\times10^{-3}$).

We were able to record CSs simultaneously from n=84 pairs of Type 1 cells, and n=89 pairs of Type 2 cells. When the primary target was in direction CS-on, Type 1 cells showed a robust synchronous response at around 90 ms latency (Fig. 5F, 2nd row), a response that was larger than Type 2 cells (Wilcoxon rank sum test; 80-110 ms post target onset, z=1.92 p=0.03). We could not perform this within

type analysis for SS synchrony because we did not have enough simultaneously recorded cells to divide the population into smaller groups.

In summary, the CSs and SSs in pairs of P-cells were on average 5x and 1.3x more likely to be synchronous than expected by chance. This temporal coordination was task dependent. During fixation of the center target, the SSs became less synchronized, but then before saccade onset SS synchrony increased and reached a peak around the time that the saccade began decelerating. In addition, CS synchrony increased both following target presentation and before saccade onset. Thus, spike timing among P-cells was regulated both during fixation and during saccades.

*Type 1 cells produced SS activity that acted as agonist while Type 2 cells produced antagonist SS activity*

The division of P-cells based on the nature of the information that they received from the olive uncovered critical differences in their SS activities. During fixation, Type 1 cells exhibited SS suppression (Fig. 6A, Wilcoxon signed rank test; -50 to 50ms post target onset, CS-on: $z=4.62$ $p=2x10^{-6}$; CS-off: $z=4.5$ $p=3x10^{-6}$), whereas in Type 2 cells the SS rates remained near baseline. During saccades both groups exhibited an SS burst, but the burst in the Type 1 group was unimodal, whereas in the Type 2 group it was bimodal, bifurcated by a pause. While in the Type 1 group the early component of the burst was stronger when the saccade was in direction CS+180, in the Type 2 group the late component of the burst appeared stronger when the saccade was in direction CS-on. Critically, the population response (CS+180 minus CS-on) in the Type 1 group showed a strong agonist burst that was then followed by a weak antagonist burst, whereas in the Type 2 group the population response lacked an agonist burst entirely but exhibited a strong antagonist burst (Fig. 6B).

In summary, the P-cells that received olivary input regarding the visual event had SSs that were suppressed during fixation, then produced an SS burst that acted as the agonist for the movement. The P-cells that received olivary input regarding movement direction were not suppressed during fixation, did not produce activity that acted as an agonist, but produced an SS burst that acted as the antagonist for the movement.

**Discussion**

We imagined that the cerebellum is akin to a schoolhouse in which the inferior olive organizes the students into classrooms where the climbing fibers are the teachers, and the P-cells are the pupils. In this framework, the information conveyed by the olivary inputs to their students provides labels that organize the P-cells into populations. Previous work had noted that while the CS rates are modulated following unexpected sensory events, they are also driven before the onset of voluntary movements (*8*, *15*, *16*, *18*, *40*, *41*), even when no sensory events trigger those movements (*14*). This raised the possibility that the olive provided sensory information to some P-cells, motor information to others. If so, a key prediction is that the climbing fibers that differ in the information that they provide will produce P-cell populations that differ in the components of behavior to which they contribute.

We found that in the oculomotor region of the vermis, the olive provided the P-cells with information regarding the direction of the visual stimulus, regardless of whether that stimulus was followed by a movement or not. Moreover, it provided information regarding the direction of the forthcoming movement, regardless of whether the movement was toward that stimulus or not. That is, the olivary input independently encoded the spatial properties of both visual and motor events.

380 Critically, the visual olivary input dominated one group of P-cells (Type 1), while the motor olivary input
381 dominated a second group (Type 2).
382 When a movement ended in error and the subject chose to correct that error, the olive
383 transmitted the error information to both groups. However, when the subject chose to suppress the
384 corrective movement, the olive reported the error direction to only one group (Type 1). This suggested
385 that sensory prediction errors were the principal teachers of Type 1 cells, while movements were the
386 principal teachers of Type 2 cells.
387 Did the SS contribution of these two groups differ? Indeed, the P-cells that received olivary input
388 regarding visual events had SSs that were suppressed during fixation, then produced a burst that likely
389 acted as an agonist to the saccade, pulling it toward the visual stimulus. On the other hand, the P-cells
390 that received olivary input regarding movements had SSs that were not suppressed during fixation.
391 These P-cells produced a burst that likely acted as an antagonist that decelerated saccades.
392
393 *Why does the olive report both sensory and motor events?*
394 The visual events in our task were random and thus can be labeled as sensory prediction errors.
395 However, the movements were voluntary actions, not errors. Why did the olivary input encode both
396 events? A critical clue is that the CSs in this region of the cerebellum arise partly from inputs that the
397 inferior olive receives from the superior colliculus (*42–44*). For example, subthreshold stimulation of a
398 region of colliculus can result in CS production (*45*). Indeed, in our data the CS response of the P-cells
399 had features that were striking similarity to the response of neurons in the superior colliculus.
400 When a target is presented in the response field of neurons in the superior colliculus (of
401 macaques), there is a bimodal response with peaks at 60 and 110 ms (*46*). This bimodal response was
402 also present with identical timing in the CS response (of marmosets). Before saccade onset, the collicular
403 neurons exhibit a gradual buildup, with a rise that is slower and a peak that is smaller for long RT
404 saccades (*47*). Both phenomena were also present in the CS response. Neurons in the superficial layers
405 of the superior colliculus respond mainly to visual events rather than movements (*48*), whereas neurons
406 in the deeper layers respond more to movements rather than visual events (*32*, *49*). Here we found that
407 the CS response differentiated two groups of P-cells, one more responsive to visual events, the other
408 more responsive to movements.
409 Finally, the response of collicular neurons to visuomotor events depends not just on the location
410 of the target, but also the reward value assigned to that stimulus (*50*). For example, the movement
411 related activity of collicular neurons is smaller when that movement is reward irrelevant (*51*). This is
412 consistent with our observation of weaker CS modulation for task irrelevant saccades. When we
413 devalued the secondary target and the animal chose to suppress the secondary saccade, the CS rate
414 modulation was present in Type 1 cells but absent in Type 2 cells. This is also consistent with a reduced
415 stimulus value producing smaller activation of the visuomotor collicular cells, and suppression of
416 movement completely silencing the motor collicular cells.
417 This might imply that the olivary input is not reporting errors, but rather the visuomotor activity
418 of neurons in the colliculus. However, this is probably not the case. If the CS response is simply a
419 stochastic mapping from one region of the superior colliculus to the cerebellum, then there is no reason
420 to expect that following saccade end there should be CS suppression. In contrast, we found that when
421 the saccade ended and there was no error, the CS response was generally suppressed. Critically, if the

saccade was in direction CS-on and at saccade end the target was not on the fovea, the omission of the expected sensory event appeared to affect the olivary input by deeply suppressing the CS response. These results suggest, but do not prove, that the CS response is partly a reflection of sensory and motor events as reported from the colliculus to the olive, and partly a reflection of cerebellar inputs to the olive that might describe expected sensory consequences of movements.

*Why are the complex spikes present before all movements and not just before the ones that are correcting errors?*

The directional encoding provided by the olive before movements may be necessary because without it, the directional modulation of the SSs may decay and disappear. In this conjecture, the directional response of P-cells to parallel fiber input during movements is continuously maintained by the olivary input that accompanies that movement. A mechanistic explanation for how the movement related CSs may sustain the SS pattern is unknown. However, it does appear that learning often begins with a CS response to the unexpected sensory event, but as the error is eliminated the CS response does not vanish; rather it shifts to the onset of the movement (*10*). As a result, in a well-practiced behavior, the CS rates as well as CS synchrony are elevated near movement onset (*18*). Indeed, we observed that both the CS firing rates, and synchrony increased when the saccades were in direction CS-on. Perhaps these changes are required for the maintenance of the direction-dependent modulation of SSs.

A second possibility is that the purpose of the CS that accompanies a movement is not to promote learning directly, but act as a stochastic perturbation to that movement. The idea is that for many cerebellar-dependent behaviors, the cerebellum is not afforded the luxury of a teacher (*17*). In this framework, life without a teacher requires a way to stochastically change the movement, then evaluate that change to determine its utility (*52*). We recently found evidence that at least part of this mechanism may be employed by the cerebellum: CSs that occur near the onset of a saccade perturb that movement (*33*), suppressing the SSs, pulling the eyes in direction CS-on. A similar phenomenon appears to be present during reaching movements (*53*). Thus, one purpose of the CSs around movement onset may be to induce stochastic changes that provides the cerebellum the means to learn without a teacher.

*Why is motor learning faster if errors are corrected, rather than simply observed?*

During motor learning it is possible to perform an action, observe the erroneous sensory consequences, but withhold the correction (*24*, *25*). The result is that the prediction error produces much smaller adaptive changes in behavior as compared to when the correction is permitted. Our results provide an explanation for this interesting phenomenon: the CS response to error is present without a corrective movement, but muted because the Type 2 cells that depend on motor information are effectively excluded from the learning process.

*A role for the cerebellum while holding still*

Holding still is an active process, requiring precise balance and sustained activation of antagonist muscles (*54*). Holmes (*55*) noted that a major symptom of cerebellar damage is the loss of muscle tone, as manifested during the process of holding still. Indeed, a recent report demonstrated that optogenetic excitation of P-cells in vermis lobules IV/V/VI during standing results in postural collapse (*56*). Here, we

464 found that the SS rates were suppressed below baseline during reward-relevant fixations in Type 1 cells,
465 but not when fixations were reward-irrelevant. Thus, it appears that the oculomotor region of the
466 vermis plays an active role both during control of saccades, and during control of fixation (*57*, *58*). Our
467 observation may be relevant for a recently reported clinical symptom termed "fixation nystagmus" in
468 which patients exhibit nystagmus while fixating a visual target, but not during other periods of fixation
469 (*59*).
470
471 *A role for the cerebellum while moving*
472 The onset of the visual target modulated the CS rates but was undetectable in the SS rates. Rather, the
473 SS rates were modulated only during movements. During saccades, the downstream effects of SS
474 modulation may be inferred based on the CS-on direction of the parent P-cell because the CS-on
475 direction tends to be aligned with the direction of action of its downstream nucleus neuron (*6*, *60*, *61*).
476 For example, during a saccade, a brief SS suppression of a P-cell pulls the eyes in the CS-on direction of
477 that cell (*33*). Thus, the information encoded in the complex spikes is critical for deciphering the
478 downstream effects of the simple spikes.
479 During a saccade, for one group of P-cells the movement is in direction CS-on, while for another
480 group that same movement is in direction CS+180. The downstream effects of their SSs will oppose each
481 other. We used this logic to compute a population response and found that before saccade onset the
482 activity in the agonist population dominated, but just before the saccade began decelerating, the
483 balance shifted to the antagonist population. As a result, the SS response resembled an
484 agonist/antagonist command. Notably, as saccade vigor changed, the antagonist activity became
485 stronger, but not the agonist activity.
486 There are several questions that remain: why the P-cells that received predominantly visual
487 information from the olive (Type 1 cells) had an SS response that acted as an agonist, pulling the eyes
488 toward that same direction, and why the P-cells that received predominantly motor information from
489 the olive (Type 2 cells) had an SS response that acted as an antagonist, stopping the saccade. If the
490 olivary input is indeed the teacher, how do these SS patterns emerge? These questions await further
491 investigation.
492
493

494 **Methods**

495 Data were collected from two marmosets (*Callithrix Jacchus*, male and female, 350-370 g, subjects M
496 and R, 6 years old) during a 2.5 year period. The marmosets were born and raised in a colony that Prof.
497 Xiaoqin Wang has maintained at the Johns Hopkins School of Medicine since 1996. The procedures on
498 the marmosets were approved by the Johns Hopkins University Animal Care and Use Committee in
499 compliance with the guidelines of the United States National Institutes of Health.

500 *Data acquisition*

501 Following recovery from head-post implantation surgery, the animals were trained to make saccades to
502 visual targets and rewarded with a mixture of applesauce and lab diet (*26*). Visual targets were
503 presented on an LCD screen (Curved MSI 32" 144 Hz - model AG32CQ) while binocular eye movements
504 were tracked using an EyeLink-1000 eye tracking system (SR Research, USA). Timing of target
505 presentations on the video screen was measured using a photo diode.

506 We performed MRI and CT imaging on each animal and used the imaging data to design an alignment
507 system that defined trajectories from the burr hole to various locations in the cerebellar vermis (*26*),
508 including points in lobule VI and VII. We used a piezoelectric, high precision microdrive (0.5 micron
509 resolution) with an integrated absolute encoder (M3-LA-3.4-15 Linear smart stage, New Scale
510 Technologies) to advance the electrode.

511 We recorded from the cerebellum using quartz insulated 4 fiber (tetrode) or 7 fiber (heptode) metal
512 core (platinum/tungsten 95/05) electrodes (Thomas Recording), and 64 channel checkerboard or linear
513 high density silicon probes (M1 and M2 probes, Cambridge Neurotech). We connected each electrode to
514 a 32 or 64 channel head stage amplifier and digitizer (RHD2132 and RHD2164, Intan Technologies, USA),
515 and then connected the head stage to a communication system (RHD2000 Evaluation Board, Intan
516 Technologies, USA). Data were sampled at 30 kHz and band-pass filtered (2.5 - 7.6 kHz). We used
517 OpenEphys (*62*) for electrophysiology data acquisition, and then used P-sort (*63*) to identify the simple
518 and complex spikes in the heptodes and tetrodes recordings, and Kilosort and Phi (*64*) to identify the
519 spikes for the silicon probes.

520 Our data was composed of n=389 P-cells that were identified because of the presence of CSs. Among
521 these neurons, we also had excellent isolation of SSs in n=257 P-cells. Thus, the data set consisted of 257
522 complete P-cells, and 389 CS only P-cells. Included in this data were n=265 CS only P-cells in the session
523 in which the corrective saccade was required, and from n=139 CS only P-cells in the session in which the
524 corrective saccade was optional. The data for the session in which the corrective saccade was required
525 were partially analyzed in a previous report (*29*).

526 *Behavioral protocol*

527 Each trial began with fixation of a center target for 200 ms (Fig. 1A), after which a primary target
528 (0.5x0.5 deg square) appeared at one of 8 randomly selected directions at a distance of 5-6.5 deg (50
529 cells were recorded during sessions with 4 random directions). The onset of the primary target coincided
530 with presentation of a distinct tone. As the animal made a saccade to this primary target, that target
531 was erased, and a secondary target was presented at a distance of 2-2.5 deg, also at one of 8 randomly
532 selected directions (4 directions for 50 cells). To assign value to this erroneous outcome, in 51% of the
533 sessions reward required both the primary and the corrective saccades, whereas in the remaining

534 sessions reward required only the primary saccade. If reward did not require the corrective saccade, the
535 secondary target was presented only briefly, returning to the primary location following ~120 ms
536 (adjusted during the recording session so that around 40% of the trials would produce a corrective
537 saccade). Following the presentation of reward, and the center target was redisplayed.

538 *Data analysis*

539 All saccades, regardless of whether they were instructed by presentation of a visual target or not, were
540 identified using a velocity threshold. Saccades to primary, secondary, and central targets were labeled as
541 targeted saccades, while all remaining saccades were labeled as task irrelevant. For the targeted
542 saccades we computed the neurophysiological response to the presentation of the visual stimulus, as
543 well as the response to the onset of the saccade. To compute the visual response to the secondary
544 target, we aligned the data to the offset of the preceding primary saccade. For task irrelevant saccades,
545 there were no visual targets and thus the response was aligned only to saccade onset.

546 The firing rates, as well as synchrony, were measured with respect to baseline. For SS rates and SS
547 synchrony, baseline was defined as a period in which the subject was not performing a saccade and was
548 not fixating the center target. We chose this period to be 200 to 100 ms before the onset of task
549 irrelevant saccades during which time the subject was fixating a random location. For complex spikes,
550 baseline rates were computed by dividing the total number of spikes by the duration of the entire
551 recording. Instantaneous firing rates were calculated from peri-event time histograms with 1 ms bin
552 size. We used a Savitzky–Golay filter (2nd order, 31 datapoints) to smooth the traces for visualization
553 purposes.

554 CS directional tuning was computed by measuring the CS firing rates following target onset as a function
555 of target angle with respect to the actual position of the eyes. We counted the number of CSs after
556 target onset up to saccade onset or a fixed 200 ms window, whichever happened first. Dividing the spike
557 count by the duration of time resulted in the CS firing rate as a function of target direction. A vector sum
558 across the directions produced a vector that we labeled CS-on.

559 To compute SS population response during saccades, we began by computing the change in SS firing
560 rate of each P-cell with respect to its baseline. Next, we labeled each saccade by measuring its direction
561 of movement with respect to the CS-on of the P-cell. Finally, we summed the activities in all P-cells (i.e.,
562 changes with respect to baseline) for saccades in direction CS-on, CS+45, etc., using a bin size of ±25
563 deg.

564 *Synchrony analysis*

565 With multi-channel electrodes, the activity of one neuron can easily be present on multiple channels,
566 thus giving the illusion that the two channels are picking up two distinct neurons. To guard against this,
567 we waveform triggered the data recorded by channel A by the spikes recorded on channel B. This
568 identified the waveform of the neuron recorded by channel B on the spike recorded on channel A. We
569 compared this cross-channel triggered waveform with the within channel triggered waveform generated
570 by the spikes recorded by channel A. The cross-channel triggered waveform must produce a different
571 cluster of spikes in A than the main neuron isolated by A. If there were spikes that occurred within 1 ms
572 of each other on channels A and B, we used these coincident-spike events to trigger the waveform in A.

The spikes in A that were identified to be coincident with B should look approximately the same as the non-coincident spikes in A. Examples of this approach are provided in Sedaghat-Nejad et al. (*26*).

Second, we jittered the spike timing for each pair of cells to produce a measure of chance level synchrony. We followed the interval jittering procedures described in (*38*): the entire recording was divided into 20 ms intervals and spikes were moved within their designated interval. We jittered each recording 50 times and computed the chance level probabilities.

To compute synchrony, we aligned the trials to visual or motor events and then at each time bin computed the quantity defined in Eq. (1) (*39*). This measure quantified the probability of coincident spikes with respect to that expected from two independent neurons. We used a 1 ms time bin to compute SS synchrony, and a 4 ms time bin to compute CS synchrony. Next, to measure task related change in synchrony, for each cell pair we measured synchrony with respect to its baseline: $s(t) - s_0$, where $s_0$ is the baseline synchrony for that cell pair as measured during a task irrelevant period of the task (same period for which baseline SS rates were measured, 200-100 ms period before task irrelevant saccades, i.e., fixation of a random location).

*Statistics*

To statistically analyze the population data, we computed p-values using a non-parametric method: Wilcoxon rank sum.

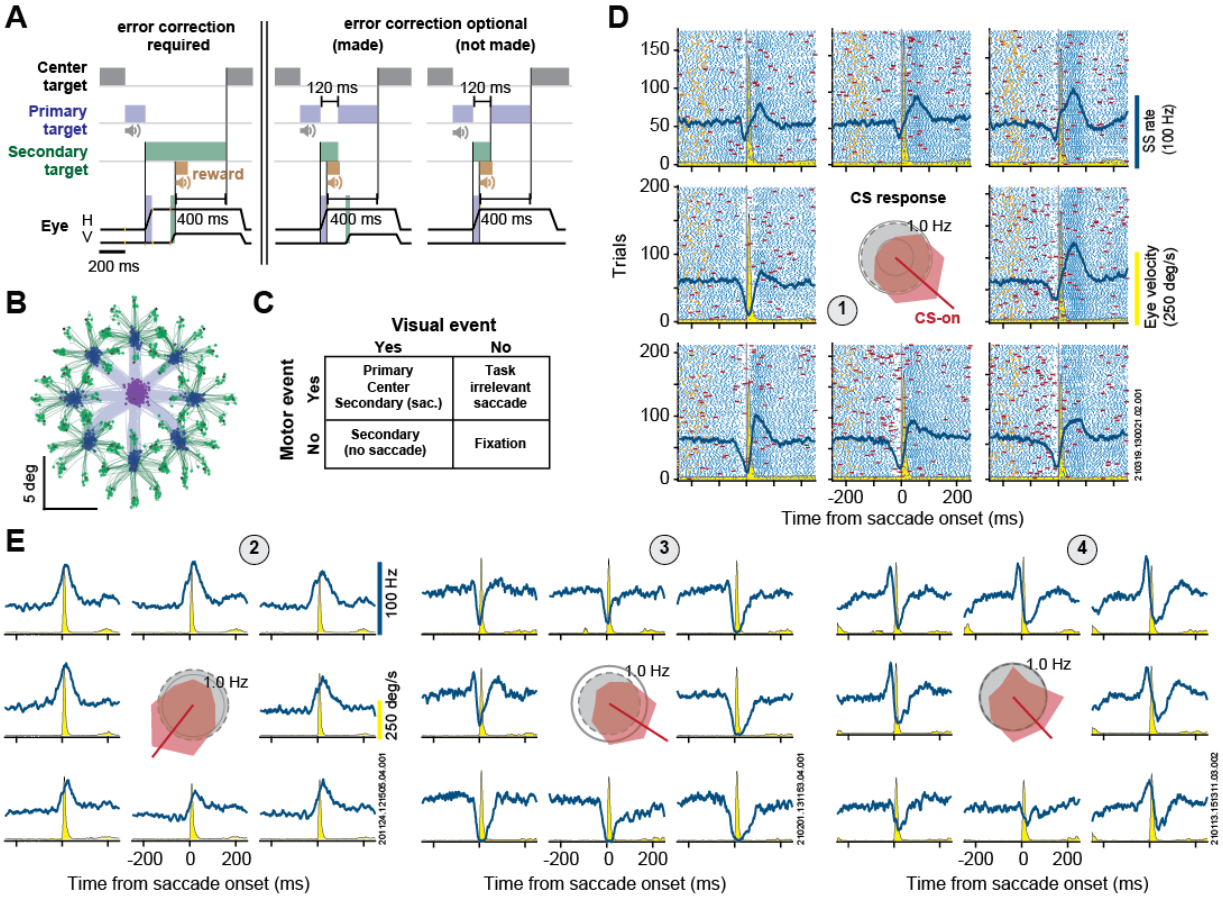


**Figure 1. A saccade task designed to dissociate sensory and motor events.** A. Task design. In some sessions the primary saccade concluded with an error and reward required correction via a secondary saccade. In other sessions this correction was optional as the reward was provided with the primary saccade. B. Saccade trajectories for primary (blue) and secondary (green) saccades. C. 2x2 design. Some but not all visual events were followed by a movement, and some but not all movements were preceded by a visual event. D. Spiking of an example P-cell. CSs (red) and SSs (blue) of a P-cell are aligned to the onset of the primary saccade. The average CS rates before saccade onset as a function of direction is shown at center. Gray circle in the center plot indicates average CS rate during entire recording. The yellow trace is saccade velocity. E. Example of P-cells with similar CS tuning (cells 1, 3, and 4) but rather different SS patterns.

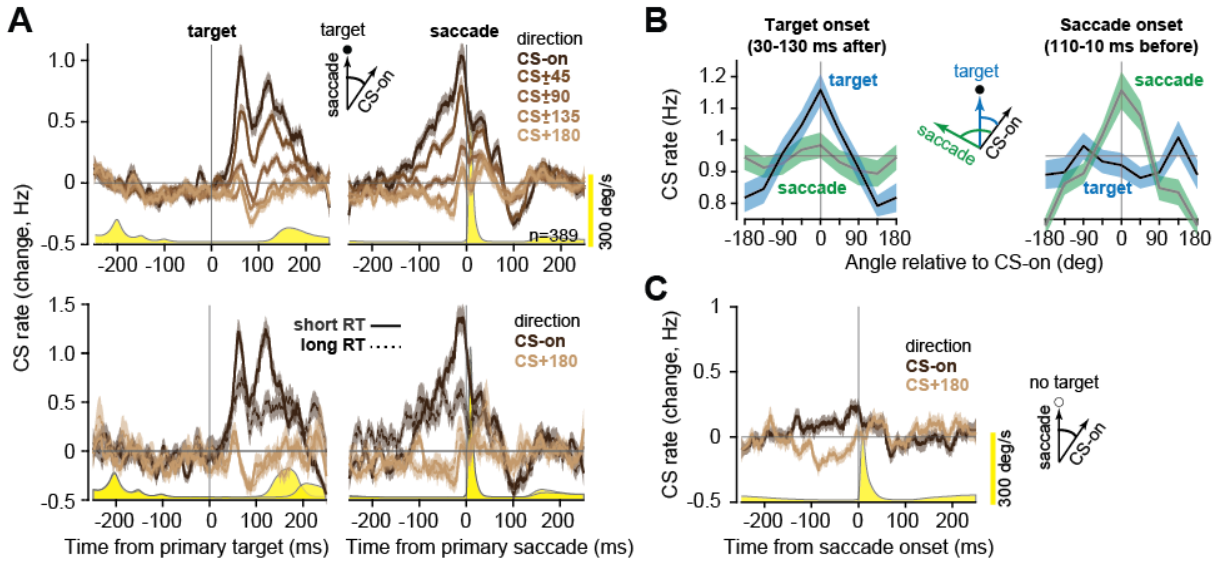


**Figure 2**. **The olivary input reported both the direction of a visual target and the direction of a forthcoming saccade**. A. CS response of the population following the onset of the primary target, and before the onset of the primary saccade. The directions of the visual and motor events are with respect to CS-on. The plot in the second row illustrates the CS response in trials that exhibited short or long reaction times (RT). Yellow trace is saccade velocity. B. In some trials the target was presented but the subject chose to saccade elsewhere. The CS response following target onset encoded target direction, but the CS response before movement onset encoded saccade direction. C. Some saccades were not preceded by the onset of a visual stimulus and were reward irrelevant. Nevertheless, the CS rates were weakly modulated before these saccades as a function of the direction of the forthcoming movement. Error bars are SEM.

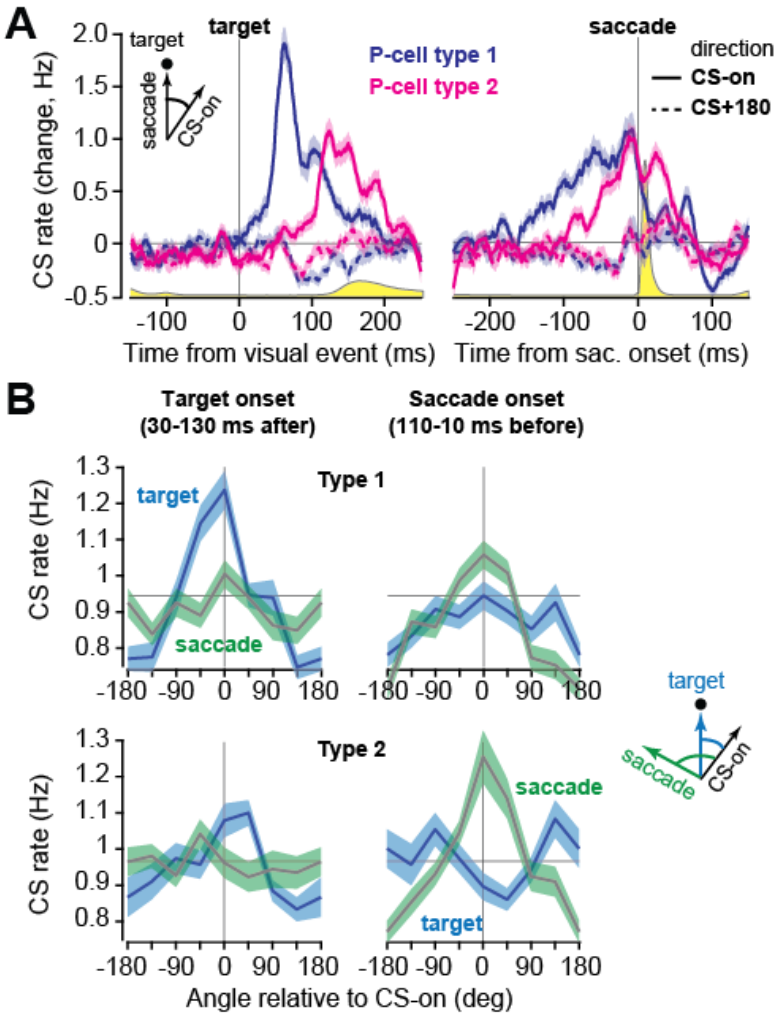


**Figure 3. One group of P-cells received information from the olive principally concerning the visual target, while another group received information principally concerning the forthcoming movement**. A. The CS response of each group of P-cells aligned to the presentation of the primary target, and aligned to the onset of the primary saccade. Type 1 P-cells had a strong early response to the visual event, but not Type 2. B. Trials in which the subject was presented with a visual target but chose to saccade elsewhere. The plots show the CS rate as a function of target direction, or saccade direction, with respect to CS-on. The CS response in Type 1 P-cells encoded the direction of the target, and only weakly the direction of the forthcoming movement. In contrast, the CS response in Type 2 P-cells encoded the forthcoming movement, and only weakly the visual event. Error bars are SEM.

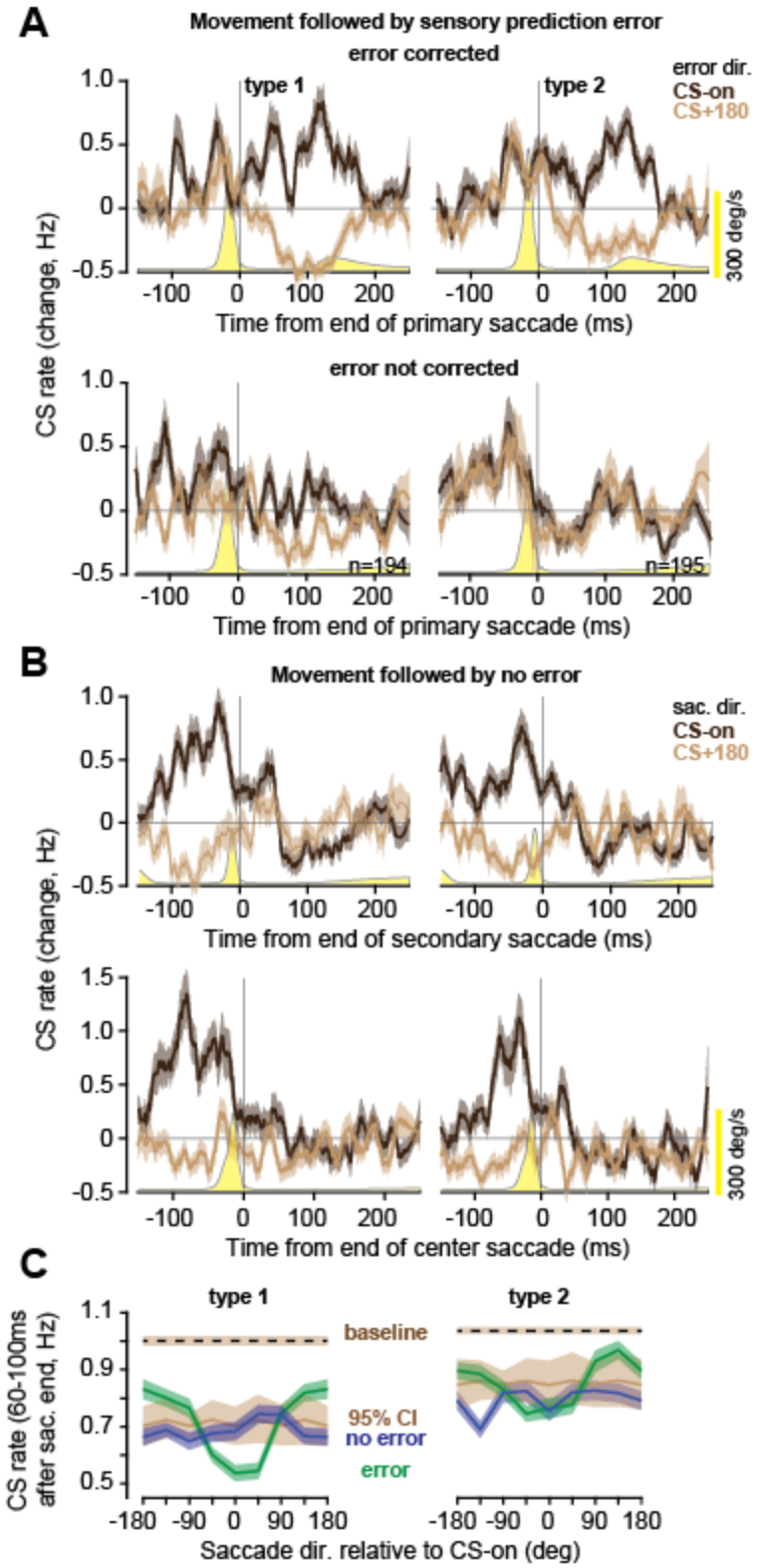


**Figure 4**. **The direction of the sensory prediction error was transmitted to the Type 1 P-cells but not Type 2**. A. At the end of the primary saccade, the target was not on the fovea, but moved to a random secondary location. Top row: trials in which the subject chose to make the secondary saccade. Data are aligned to end of the primary saccade. Both P-cell groups had a CS response that reported the direction of the error. Bottom row: trials in which the subject chose to suppress the secondary saccade. In Type 1 P-cells the CS response (weakly) reported the direction of error, but not in Type 2 P-cells. Yellow trace is saccade velocity. B. The CS response following saccades that did not experience an error (secondary and center saccades). Error bars are SEM. C The CS firing rates in the 60-100ms following completion of the saccade as a function of the direction of that saccade. Data are shown for Type 1 and Type 2 cells, for saccades that experienced endpoint error (primary saccades, green), and saccades that did not experience endpoint error (secondary and center saccades, blue). Baseline CS rates are indicated. 95% confidence interval was generated by removing direction labels for the primary saccades. Error bars are SEM.

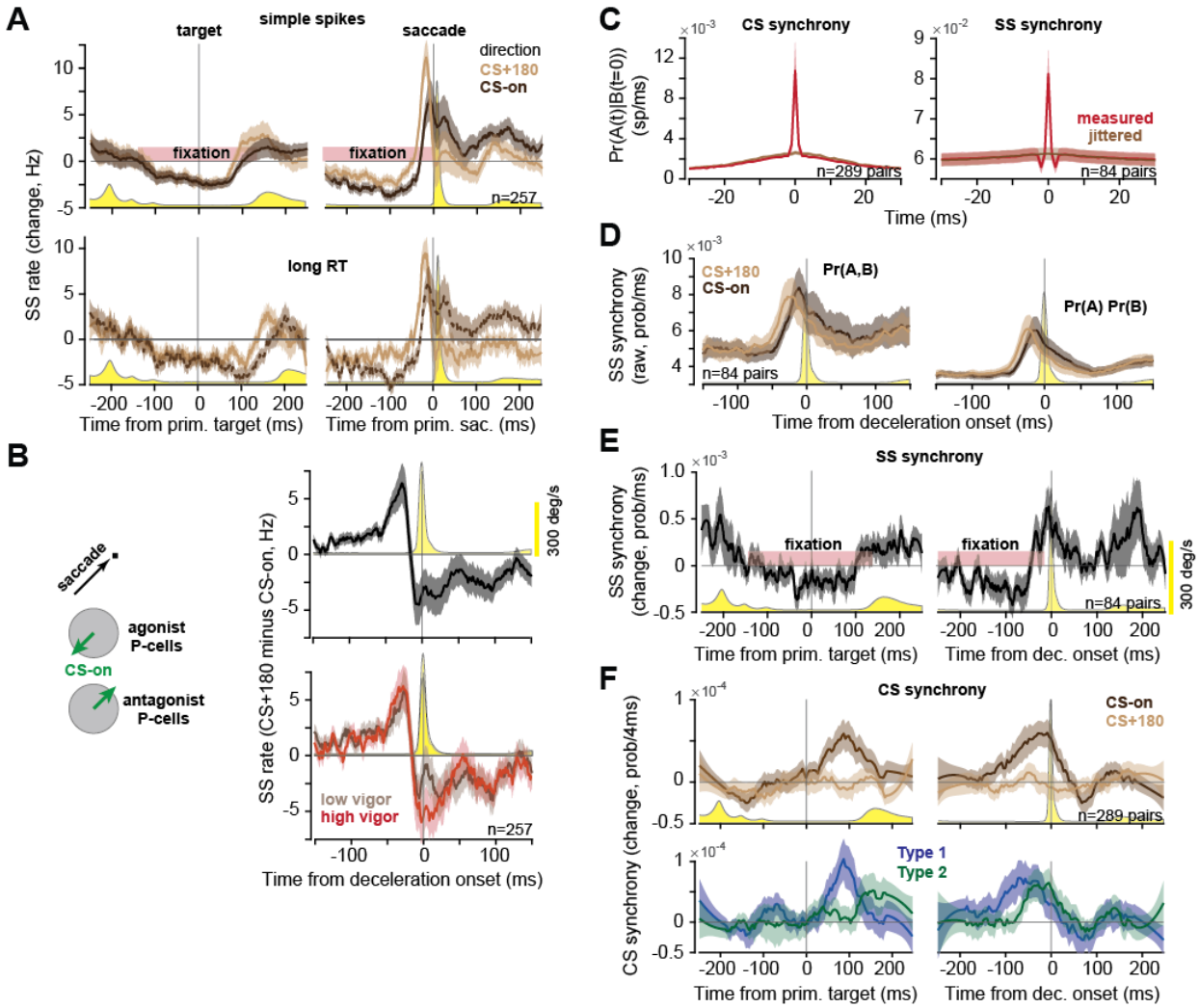


**Figure 5**. **Simple spikes were suppressed during fixation and then exhibited an agonist-antagonist burst during saccades. Spikes were more synchronized during saccades.** A. Top row: SS activity aligned to the onset of the primary target and saccade. Bottom row: SS activity in trials that exhibited long reaction times (RT). There is little or no response to the visual event, but a burst in response to the motor event. The burst is stronger and occurs earlier for saccades in direction CS+180. Yellow trace is saccade velocity. Error bars are SEM. B. When a saccade takes place at an arbitrary direction, for one group of P-cells that saccade is in direction CS-on, while for another group the same saccade is in direction CS+180. The population response is the SS rates in direction CS+180 minus CS-on. The result is an agonist-antagonist burst. High vigor saccades have a larger antagonist SS burst. Error bars are SEM. C. SS and CS synchrony. The plot shows $\Pr(A(t) = 1|B(0) = 1)$, i.e., the probability of spiking in neuron A at time t, given that neuron B spiked at time 0 (using a 1 ms time bin). Chance was estimated via spike time jittering (20 ms intervals). Error bars are 99% confidence intervals. Time bin is 1 ms. D. SS raw synchrony $\Pr\,(A, B)$ and chance synchrony $\Pr(A)\,\Pr(B)$ for primary saccades. Time bin is 1 ms. Error bars are SEM. E. SS and CS synchrony, measured via Eq. (1). SS synchrony time bin is 1 ms. CS time bin is 4 ms. Error bars are SEM.

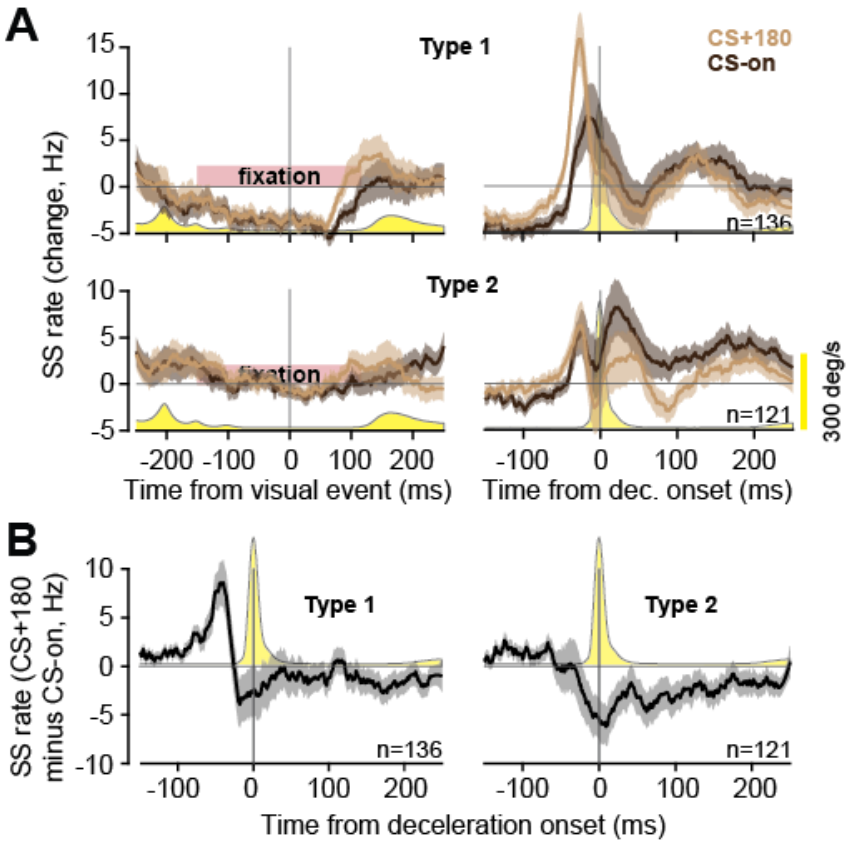


**Figure 6. Type 1 P-cells produced an agonist SS burst while Type 2 P-cells produced an antagonist burst**. A. SS activities in each group of P-cells in response to the visual and motor events. During fixation the SS rates were suppressed in Type 1 but not Type 2. During saccades, in Type 1 the burst was earlier and larger in direction CS+180 before saccade onset, but in Type 2 the burst was larger in direction CS-on after deceleration onset. B. SS rates in direction CS+180 minus CS-on. Positive values can be interpreted as commanding downstream forces in the direction of the saccade (agonist). Negative values can be interpreted as commanding downstream forces opposite to the direction of the saccade (antagonist).

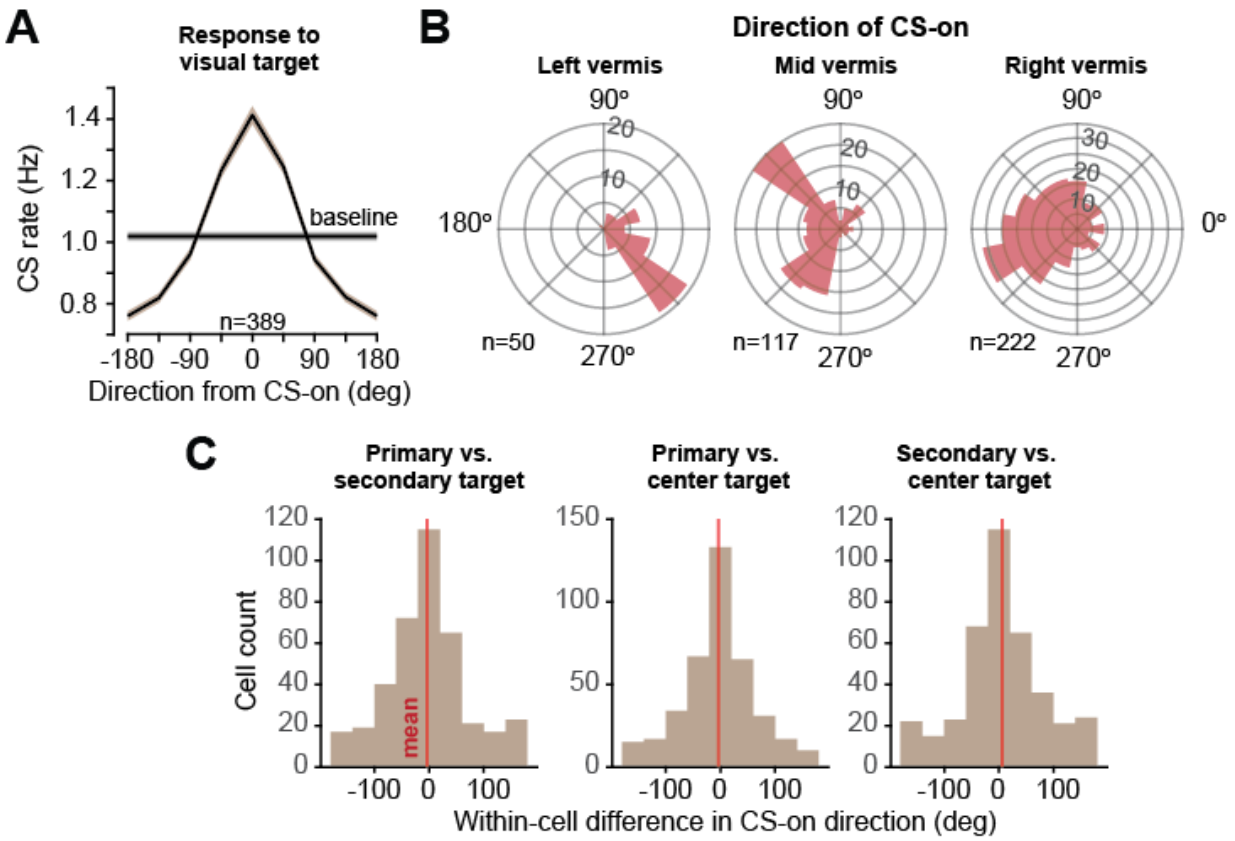


**Supplementary Fig. S1.** The direction of CS-on remained consistent in response to various targets but varied with location of the P-cell in the vermis. **A**. Average CS firing rates following the presentation of the primary target, as a function of direction, aligned to direction CS-on. Error bars are SEM. **B**. Distribution of CS-on as a function of location of recording in the vermis. Bin size is 15°, and the wedge at each bin represents the number of P-cells with that CS-on. P-cells tended to have a CS-on toward the contralateral hemifield. **C**. Within cell difference between CS-on directions as computed following the onset of the primary target, the secondary target, and the center target. We found no systematic differences in the estimate of CS-on between various types of targets, and thus combined the response for all targets to compute the CS-on of each P-cell.

709 1. M. Ito, M. Sakurai, P. Tongroach, Climbing fibre induced depression of both mossy fibre
710 responsiveness and glutamate sensitivity of cerebellar Purkinje cells. *J.Physiol*. **324**, 113–134
711 (1982).

712 2. J. J. Kim, D. J. Krupa, R. F. Thompson, Inhibitory cerebello-olivary projections and blocking effect in
713 classical conditioning. *Science*. **279**, 570–573 (1998).

714 3. J. F. Medina, S. G. Lisberger, Links from complex spikes to local plasticity and motor learning in the
715 cerebellum of awake-behaving monkeys. *Nat.Neurosci.* **11**, 1185–1192 (2008).

716 4. Y. Yang, S. G. Lisberger, Role of Plasticity at Different Sites across the Time Course of Cerebellar
717 Motor Learning. *J. Neurosci.* **34**, 7077–7090 (2014).

718 5. D. J. Herzfeld, Y. Kojima, R. Soetedjo, R. Shadmehr, Encoding of action by the Purkinje cells of the
719 cerebellum. *Nature*. **526**, 439–442 (2015).

720 6. D. J. Herzfeld, Y. Kojima, R. Soetedjo, R. Shadmehr, Encoding of error and learning to correct that
721 error by the Purkinje cells of the cerebellum. *Nat.Neurosci.* **21**, 736–743 (2018).

722 7. A. S. Fanning, A. M. Shakhawat, J. L. Raymond, Population calcium responses of Purkinje cells in
723 the oculomotor cerebellum driven by nonvisual input. *J. Neurophysiol.* **126**, 1391–1402 (2021).

724 8. S. Kitazawa, T. Kimura, P. B. Yin, Cerebellar complex spikes encode both destinations and errors in
725 arm movements. *Nature*. **392**, 494 (1998).

726 9. R. Soetedjo, A. F. Fuchs, Complex spike activity of purkinje cells in the oculomotor vermis during
727 behavioral adaptation of monkey saccades. *J Neurosci*. **26**, 7741–7755 (2006).

728 10. S. Ohmae, J. F. Medina, Climbing fibers encode a temporal-difference prediction error during
729 cerebellar learning in mice. *Nat.Neurosci.* **18**, 1798–1803 (2015).

730 11. C. Ju, L. W. J. Bosman, T. M. Hoogland, A. Velauthapillai, P. Murugesan, P. Warnaar, R. M. van
731 Genderen, M. Negrello, C. I. D. Zeeuw, Neurons of the inferior olive respond to broad classes of
732 sensory input while subject to homeostatic control. *J. Physiol.* **597**, 2483–2514 (2019).

733 12. N. Larry, M. Yarkoni, A. Lixenberg, M. Joshua, Cerebellar climbing fibers encode expected reward
734 size. *eLife*. **8** (2019), doi:10.7554/eLife.46870.

735 13. L. Bina, V. Romano, T. M. Hoogland, L. W. J. Bosman, C. I. De Zeeuw, Purkinje cells translate
736 subjective salience into readiness to act and choice performance. *Cell Rep.* **37**, 110116 (2021).

737 14. J. P. Welsh, E. J. Lang, I. Suglhara, R. Llinas, Dynamic organization of motor control within the
738 olivocerebellar system. *Nature*. **374**, 453–457 (1995).

739 15. A. L. Hewitt, L. S. Popa, T. J. Ebner, Changes in Purkinje cell simple spike encoding of reach
740 kinematics during adaption to a mechanical perturbation. *J.Neurosci.* **35**, 1106–1124 (2015).

741 16. T. M. Hoogland, J. R. De Gruijl, L. Witter, C. B. Canto, C. I. De Zeeuw, Role of Synchronous
742 Activation of Cerebellar Purkinje Cell Ensembles in Multi-joint Movement Control. *Curr. Biol.* **25**,
743 1157–1165 (2015).

744 17. W. Heffley, E. Y. Song, Z. Xu, B. N. Taylor, M. A. Hughes, A. McKinney, M. Joshua, C. Hull,
745 Coordinated cerebellar climbing fiber activity signals learned sensorimotor predictions. *Nat.*
746 *Neurosci.* **21**, 1431–1441 (2018).

747 18. M. J. Wagner, J. Savall, O. Hernandez, G. Mel, H. Inan, O. Rumyantsev, J. Lecoq, T. H. Kim, J. Z. Li, C.
748 Ramakrishnan, K. Deisseroth, L. Luo, S. Ganguli, M. J. Schnitzer, A neural circuit state change
749 underlying skilled movements. *Cell*. **184**, 3731-3747.e21 (2021).

750 19. R. Apps, M. Garwicz, Anatomical and physiological foundations of cerebellar information
751 processing. *Nat.Rev.Neurosci.* **6**, 297–311 (2005).

752 20. F. Najafi, A. Giovannucci, S. S. Wang, J. F. Medina, Coding of stimulus strength via analog calcium
753 signals in Purkinje cell dendrites of awake mice. *eLife*. **3**, e03663 (2014).

754 21. R. Soetedjo, Y. Kojima, A. F. Fuchs, Complex spike activity in the oculomotor vermis of the
755 cerebellum: a vectorial error signal for saccade motor learning? *J.Neurophysiol.* **100**, 1949–1966
756 (2008).

757 22. D. J. Calame, M. I. Becker, A. L. Person, Cerebellar associative learning underlies skilled reach
758 adaptation. *Nat. Neurosci.*, 1–12 (2023).

759 23. T. Ishikawa, S. Tomatsu, Y. Tsunoda, J. Lee, D. S. Hoffman, S. Kakei, Releasing dentate nucleus cells
760 from Purkinje cell inhibition generates output from the cerebrocerebellum. *PLoS.One.* **9**, e108774
761 (2014).

762 24. J. Wallman, A. F. Fuchs, Saccadic gain modification: visual error drives motor adaptation. *J*
763 *Neurophysiol*. **80**, 2405–2416 (1998).

764 25. Y. W. Tseng, J. Diedrichsen, J. W. Krakauer, R. Shadmehr, A. J. Bastian, Sensory prediction errors
765 drive cerebellum-dependent adaptation of reaching. *J.Neurophysiol.* **98**, 54–62 (2007).

766 26. E. Sedaghat-Nejad, D. J. Herzfeld, P. Hage, K. Karbasi, T. Palin, X. Wang, R. Shadmehr, Behavioral
767 training of marmosets and electrophysiological recording from the cerebellum. *J.Neurophysiol.*
768 **122**, 1502–1517 (2019).

769 27. K. Ohtsuka, H. Noda, Discharge properties of Purkinje cells in the oculomotor vermis during visually
770 guided saccades in the macaque monkey. *J.Neurophysiol.* **74**, 1828–1840 (1995).

771 28. P. Thier, P. W. Dicke, R. Haas, S. Barash, Encoding of movement time by populations of cerebellar
772 Purkinje cells. *Nature*. **405**, 72–76 (2000).

773 29. E. Sedaghat-Nejad, J. S. Pi, P. Hage, M. A. Fakharian, R. Shadmehr, Synchronous spiking of
774 cerebellar Purkinje cells during control of movements. *Proc. Natl. Acad. Sci.* **119**, e2118954119
775 (2022).

776 30. D. P. Munoz, R. H. Wurtz, Saccade-related activity in monkey superior colliculus. I. Characteristics
777 of burst and buildup cells. *J.Neurophysiol.* **73**, 2313–2333 (1995).

778 31. L. E. Mays, D. L. Sparks, Dissociation of visual and saccade-related responses in superior colliculus
779 neurons. *J.Neurophysiol.* **43**, 207–232 (1980).

780 32. E. C. Ayar, M. R. Heusser, C. Bourrelly, N. J. Gandhi, Distinct context- and content-dependent
781 population codes in superior colliculus during sensation and action. *Proc. Natl. Acad. Sci.* **120**,
782 e2303523120 (2023).

783 33. S. Z. Muller, J. S. Pi, P. Hage, M. A. Fakharian, E. Sedaghat-Nejad, R. Shadmehr, Complex spikes
784 perturb movements, revealing the sensorimotor map of Purkinje cells. *Curr.Biol* (in press).

785 34. Y. El-Shamayleh, Y. Kojima, R. Soetedjo, G. D. Horwitz, Selective Optogenetic Control of Purkinje
786 Cells in Monkey Cerebellum. *Neuron*. **95**, 51-62.e4 (2017).

787 35. P. Hage, I. K. Jang, V. Looi, M. A. Fakharian, S. P. Orozco, J. S. Pi, E. Sedaghat-Nejad, R. Shadmehr,
788 Effort cost of harvest affects decisions and movement vigor of marmosets during foraging (2023),
789 p. 2023.02.04.527146, , doi:10.1101/2023.02.04.527146.

790 36. J. E. Choi, P. A. Vaswani, R. Shadmehr, Vigor of movements and the cost of time in decision
791 making. *J.Neurosci.* **34**, 1212–1223 (2014).

792 37. T. R. Reppert, I. Rigas, D. Herzfeld, E. Sedaghat-Nejad, O. Komogortsev, R. Shadmehr, Movement
793 vigor as a trait-like attribute of individuality. *J.Neurophysiol.* **120**, 741–757 (2018).

794 38. J. Platkiewicz, E. Stark, A. Amarasingham, Spike-Centered Jitter Can Mistake Temporal Structure.
795 *Neural Comput.* **29**, 783–803 (2017).

796 39. D. J. Herzfeld, M. Joshua, S. G. Lisberger, Rate versus synchrony codes for cerebellar control of
797 motor behavior. *Neuron*. **111**, 2448-2460.e6 (2023).

798 40. M. Junker, D. Endres, Z. P. Sun, P. W. Dicke, M. Giese, P. Thier, Learning from the past: A
799 reverberation of past errors in the cerebellar climbing fiber signal. *PLOS Biol.* **16**, e2004344 (2018).

800 41. Y. Kobayashi, K. Kawano, A. Takemura, Y. Inoue, T. Kitama, H. Gomi, M. Kawato, Temporal firing
801 patterns of Purkinje cells in the cerebellar ventral paraflocculus during ocular following responses
802 in monkeys II. Complex spikes. *J.Neurophysiol.* **80**, 832–848 (1998).

803 42. Y. Kojima, R. Soetedjo, Elimination of the error signal in the superior colliculus impairs saccade
804 motor learning. *Proc.Natl.Acad.Sci.U.S.A*. **115**, E8987–E8995 (2018).

805 43. Y. Kojima, R. Soetedjo, Change in sensitivity to visual error in superior colliculus during saccade
806 adaptation. *Sci.Rep.* **7**, 9566 (2017).

807 44. P. J. May, S. Warren, Y. Kojima, The Superior Colliculus Projection Upon the Macaque Inferior Olive
808 (2023), , doi:10.21203/rs.3.rs-2986616/v1.

809 45. R. Soetedjo, Y. Kojima, A. F. Fuchs, How cerebellar motor learning keeps saccades accurate. *J.*
810 *Neurophysiol.* **121**, 2153–2162 (2019).

811 46. G. Yu, L. N. Katz, C. Quaia, A. Messinger, R. J. Krauzlis, Short-latency preference for faces in the
812 primate superior colliculus (2023), p. 2023.09.06.556401, , doi:10.1101/2023.09.06.556401.

813 47. R. Ratcliff, Y. T. Hasegawa, R. P. Hasegawa, P. L. Smith, M. A. Segraves, Dual diffusion model for
814 single-cell recording data from the superior colliculus in a brightness-discrimination task.
815 *J.Neurophysiol.* **97**, 1756–1774 (2007).

816 48. S. Everling, M. C. Dorris, R. M. Klein, D. P. Munoz, Role of primate superior colliculus in preparation
817 and execution of anti-saccades and pro-saccades. *J.Neurosci.* **19**, 2740–2754 (1999).

818 49. D. P. Munoz, R. H. Wurtz, Fixation cells in monkey superior colliculus. I. Characteristics of cell
819 discharge. *J.Neurophysiol.* **70**, 559–575 (1993).

820 50. T. Ikeda, O. Hikosaka, Positive and negative modulation of motor response in primate superior
821 colliculus by reward expectation. *J.Neurophysiol.* **98**, 3163–3170 (2007).

822 51. D. M. Waitzman, T. P. Ma, L. M. Optican, R. H. Wurtz, Superior colliculus neurons mediate the
823 dynamic characteristics of saccades. *J.Neurophysiol.* **66**, 1716–1737 (1991).

824 52. G. Bouvier, J. Aljadeff, C. Clopath, C. Bimbard, J. Ranft, A. Blot, J.-P. Nadal, N. Brunel, V. Hakim, B.
825 Barbour, Cerebellar learning using perturbations. *eLife*. **7**, e31599 (2018).

826 53. M. L. Streng, L. S. Popa, T. J. Ebner, Climbing Fibers Control Purkinje Cell Representations of
827 Behavior. *J.Neurosci.* **37**, 1997–2009 (2017).

828 54. R. Shadmehr, Distinct neural circuits for control of movement vs. holding still. *J.Neurophysiol.* **117**,
829 1431–1460 (2017).

830 55. G. Holmes, The cerebellum of man. *Brain*. **62**, 1–30 (1939).

831 56. A. Gouhier, V. Villette, B. Mathieu, A. Ayon, J. Bradley, S. Dieudonné, Identification and
832 organization of a postural anti-gravity module in the cerebellar vermis (2023), p.
833 2023.10.10.561555, , doi:10.1101/2023.10.10.561555.

834 57. L. Goffart, L. L. Chen, D. L. Sparks, Deficits in saccades and fixation during muscimol inactivation of
835 the caudal fastigial nucleus in the rhesus monkey. *J.Neurophysiol.* **92**, 3351–3367 (2004).

836 58. M. Takagi, D. S. Zee, R. J. Tamargo, Effects of lesions of the oculomotor vermis on eye movements
837 in primate: saccades. *J.Neurophysiol.* **80**, 1911–1931 (1998).

838 59. S.-U. Lee, H.-J. Kim, J.-Y. Choi, J.-H. Choi, D. S. Zee, J.-S. Kim, Nystagmus only with fixation in the
839 light: a rare central sign due to cerebellar malfunction. *J. Neurol.* (2022), doi:10.1007/s00415-022-
840 11108-9.

841 60. C. F. Ekerot, H. Jorntell, M. Garwicz, Functional relation between corticonuclear input and
842 movements evoked on microstimulation in cerebellar nucleus interpositus anterior in the cat.
843 *ExpBrain Res*. **106**, 365–376 (1995).

844 61. C. I. De Zeeuw, Bidirectional learning in upbound and downbound microzones of the cerebellum.
845 *Nat. Rev. Neurosci.* **22**, 92–110 (2021).

846 62. J. H. Siegle, A. C. Lopez, Y. A. Patel, K. Abramov, S. Ohayon, J. Voigts, Open Ephys: an open-source,
847 plugin-based platform for multichannel electrophysiology. *JNeural Eng*. **14**, 045003 (2017).

848 63. E. Sedaghat-Nejad, M. A. Fakharian, J. Pi, P. Hage, Y. Kojima, R. Soetedjo, S. Ohmae, J. F. Medina, R.
849 Shadmehr, P-sort: an open-source software for cerebellar neurophysiology. *J. Neurophysiol.* **126**,
850 1055–1075 (2021).

851 64. M. Pachitariu, N. Steinmetz, S. Kadir, M. Carandini, H. K. D, Kilosort: realtime spike-sorting for
852 extracellular electrophysiology with hundreds of channels. *bioRxiv*, 061481 (2016).

853
854